

## Letters

### Surface Plasmon Resonance Spectroscopy as a Probe of In-Plane Polymerization in Monolayer Organic Conducting Films

R. Georgiadis,\* K. A. Peterlinz, J. R. Rahn, A. W. Peterson, and J. H. Grassi

*Department of Chemistry, Boston University, Boston, Massachusetts 02215*

*Received December 31, 1999. In Final Form: June 21, 2000*

Several groups have shown that alkanethiol-modified pyrroles can be tethered to a gold surface, but there is often little evidence that, once oxidized, the resulting monolayer film is an organic conducting polymer. Using surface plasma resonance (SPR) spectroscopy, we demonstrate for the first time that, upon electrochemical oxidation, self-assembled alkanethiol-pyrrole films on gold show behavior characteristic of organic conducting polymers: we observe reversible changes in the optical constants of the organic film upon doping/dedoping. Since the optical constants are related to film conductivity, we show that the effective isotropic dielectric constant of the film obtained in the standard SPR data analysis can be interpreted in terms of in-plane and out-of-plane contributions to film conductivity. We find that the in-plane conductivity of oxidized 3-( $\omega$ -mercaptoundecyl)pyrrole is smaller, but of the same order of magnitude, than that found for thick films of polypyrrole. Most importantly, we observe reversible changes in the optical constants of the polymerized film, which are consistent with electrochemical switching of an organic conducting polymer whose conductivity is largest for the doped state and decreases for the dedoped state.

#### Introduction

Chemical reactions in supported molecular assemblies are important in research ranging from biology to materials science. Surface-immobilized monomers offer unique opportunities for study, optimization, and exploitation of the effect of the surface environment on the process of interest. Much use has been made of self-assembled monolayer films of alkanethiols in research as a means to promote adhesion at interfaces, to resist corrosion, and to fabricate tailored surfaces of chemical and biological sensors and molecular electronics.<sup>1</sup> Monomolecular constituents of the film, when functionalized with polymerizable moieties, can be chemically or electrochemically induced to polymerize.

One class of films that have attracted much attention due to potential applications are monomolecular alkanethiol films functionalized with a terminal pyrrole

group. Pyrrole can polymerize to form polypyrrole, an organic conducting polymer which can be switched between conducting and insulating states by reversible electrochemical doping and dedoping.<sup>2</sup> As usually grown, polypyrrole films do not adhere well to substrates, are rough and irregular, and have conductivities which are too small for most practical applications. For bulk polypyrrole, it has been shown that the conductivity can be improved when the material is grown in a more ordered, constrained geometry.<sup>3</sup>

Several groups have shown that alkanethiol-modified pyrroles can be tethered to a gold surface,<sup>4–18</sup> but there

(2) Patil, A. O.; Heeger, A. J.; Wudl, F. *Chem. Rev.* **1988**, *88*, 183–200.

(3) Menon, V. P.; Lei, J. T.; Martin, C. R. *Chem. Mater.* **1996**, *8*, 2382–90.

(4) Willicut, R. J.; McCarley, R. L. *J. Am. Chem. Soc.* **1994**, *116*, 10823–10824.

(5) Sayre, C. N.; Collard, D. M. *Langmuir* **1995**, *11*, 302–306.

(6) Willicut, R. J.; McCarley, R. L. *Adv. Mater.* **1995**, *7*, 759–762.

(7) Willicut, R. J.; McCarley, R. L. *Langmuir* **1995**, *11*, 296–301.

(1) Whitesides, G. M.; Ferguson, G. S.; Allara, D.; Scherson, D.; Speaker, L.; Ulman, A. *Crit. Rev. Surf. Chem.* **1993**, *3*, 49–65.

is often little evidence that, once oxidized, the resulting film is an organic conducting polymer. In fact, it has been noted in the literature<sup>13</sup> that there is no in situ spectroscopic evidence that a surface-bound aromatic moiety exists after anodic oxidation. McCarley et al.<sup>11</sup> have recently published ex situ RAIR (reflection absorption infrared) spectra of oxidized monolayers under an inert atmosphere, which show evidence of aromatic C–H out-of-plane deformation bands.

Optical measurements are ideal for measuring the large change in the absorptivity for organic conducting polymers upon oxidation and reversible doping.<sup>2</sup> For very thin films however, UV transmission spectroscopy lacks the sensitivity required. The high sensitivity of surface plasmon resonance, SPR, spectroscopy to optically absorbing films has been documented<sup>19–21</sup> but has been underutilized. SPR is also well suited for electrochemical studies of absorbing films, provided that the effect of the electrochemical field is properly accounted for.<sup>22</sup>

In this paper, we demonstrate the feasibility of measuring the optical constants of absorbing films in situ using surface plasmon resonance spectroscopy. We observe a distinct change in the SPR spectroscopy data for self-assembled monolayers of 3-( $\omega$ -mercaptoundecyl)pyrrole before and after electrochemical oxidation. More importantly, the optical absorptivity of these oxidized films undergoes a reversible change upon doping/dedoping, as expected for an organic conducting polymer film, which switches between conducting (doped) and insulating (undoped) states. Finally, we present a theoretical analysis which shows how in situ SPR data can be interpreted to obtain the in-plane component of the dielectric constant of an anisotropic film, a quantity which can be related to in-plane conductivity.

### Experimental Section

An SPR spectrometer of the Kretschmann configuration employing a 632.8 nm He/Ne laser was used. Details of the apparatus have been described previously.<sup>23</sup> For electrochemical SPR,<sup>22</sup> the gold surface was used as both a working electrode surface and the SPR substrate. The SPR solution cell allows insertion of electrodes to produce a standard three-electrode cell.

All solutions were prepared with Nanopure water (18 M $\Omega$  cm, Barnstead) and deaerated with dry nitrogen for approximately 10 min prior to use. Anhydrous propylene carbonate and HPLC grade ethanol were used as received from Aldrich. Electrolyte solutions were prepared using tetrabutylammonium perchlorate (TBAP) (electrochemical grade, Fluka) and perchloric acid

(8) Wurm, D. B.; Brittain, S. T.; Kim, Y. T. *Langmuir* **1996**, *12*, 3756–3758.

(9) Collard, D. M.; Sayre, C. N. *Synth. Met.* **1997**, *84*, 329–332.

(10) Sayre, C. N.; Collard, D. M. *Langmuir* **1997**, *13*, 714–722.

(11) McCarley, R. L.; Willicut, R. J. *J. Am. Chem. Soc.* **1998**, *120*, 9296–9304.

(12) Smela, E. *Langmuir* **1998**, *14*, 2996–3002.

(13) Smela, E.; Kariis, H.; Yang, Z. P.; Mecklenburg, M.; Liedberg, B. *Langmuir* **1998**, *14*, 2984–2995.

(14) Smela, E.; Kariis, H.; Yang, Z. P.; Uvdal, K.; Zuccarello, G.; Liedberg, B. *Langmuir* **1998**, *14*, 2976–2983.

(15) Smela, E.; Zuccarello, G.; Kariis, H.; Liedberg, B. *Langmuir* **1998**, *14*, 2970–2975.

(16) Wurm, D. B.; Zong, K.; Kim, Y. H.; Kim, Y. T.; Shin, M.; Jeon, I. C. *J. Electrochem. Soc.* **1998**, *145*, 1483–1488.

(17) Kim, Y. H.; Kim, Y. T. *Langmuir* **1999**, *15*, 1876–1878.

(18) Wang, J.; Zeng, B. Z.; Fang, C.; He, F.; Zhou, X. Y. *Electroanalysis* **1999**, *11*, 1345–1349.

(19) Pockrand, I.; Swalen, J. D.; Gordon, J. G.; Philpott, M. R. *Surf. Sci.* **1977**, *74*, 237–244.

(20) Pockrand, I. *Surf. Sci.* **1978**, *72*, 577–588.

(21) Pockrand, I.; Swalen, J. D.; Santo, R.; Brillante, A.; Philpott, M. R. *J. Chem. Phys.* **1978**, *69*, 4001–4011.

(22) Grassi, J. H.; Reilly, S. M.; Georgiadis, R. Submitted for publication in *Langmuir*.

(23) Peterlinz, K. A.; Georgiadis, R. *Langmuir* **1996**, *12*, 4731–40.

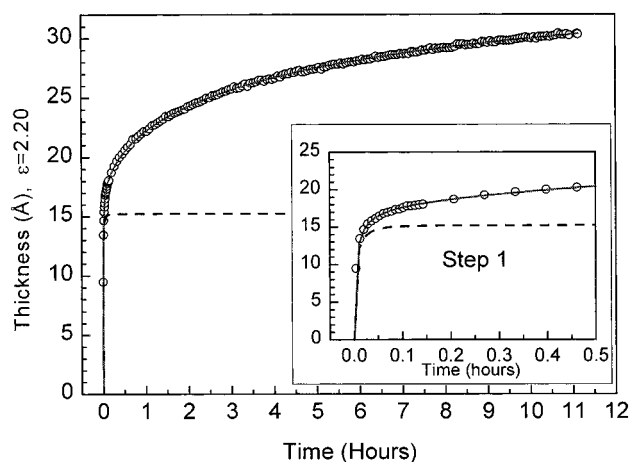


**Figure 1.** Formation kinetics for 3-( $\omega$ -mercaptoundecyl)pyrrole in ethanol. Shown is the average thickness (open circles) calculated from in situ SPR spectra measured during film formation assuming the dielectric constant  $\epsilon = 2.20$ . The solid line through the data shows a fit using a model which assumes two concerted kinetic steps; the dashed line indicates the first kinetic step alone.

(Optima grade, Fisher). 3-( $\omega$ -Mercaptoundecyl)pyrrole<sup>5,10</sup> was provided by Professor David Collard (Georgia Tech).

Self-assembled films of 3-( $\omega$ -mercaptoundecyl)pyrrole were prepared by exposing the gold-coated hemicylindrical prism to 1 mM 3-( $\omega$ -mercaptoundecyl)pyrrole in ethanol for 60 h. The film was rinsed with neat ethanol and water and placed in a deaerated 0.1 M perchloric acid aqueous solution for the electrochemical experiments.

All electrochemical potentials are referenced to Ag/AgCl using an EG&G 263A potentiostat. For the electrochemical oxidation, the cyclic voltammogram was initially set to a potential of 0.15 V and was cycled to 0.9 V at 100 mV/s. SPR measurements were made with the potential fixed at either 0.15 or 0.9 V. After the completion of the cyclic voltammogram scans in aqueous solution, the gold electrode was rinsed with water, ethanol, deaerated propylene carbonate, and 0.1 M TBAP in propylene carbonate. The SPR data were collected after each rinse. Electrochemical doping experiments were carried out by cycling the voltage between 0.15 and 0.9 V while the film was in contact with a deaerated solution of 0.1 M TBAP in propylene carbonate.

### Data Analysis

The SPR angular reflectance data are fit to the full Fresnel equations using the nonlinear least-squares optimization tools provided by MatLab and techniques described previously.<sup>23,22</sup> The spectrometer is calibrated from fitting the SPR response in water prior to electrochemical experiments to determine the absolute angle of incidence. These measurements are analyzed to determine the optical constants of the metal substrate. For data obtained at a static electrochemical potential, the data are analyzed as previously discussed; however, to compare results obtained at different potentials, the data analysis is modified to take into account the effect of the applied electrochemical field on the optical constants of the gold substrate.<sup>22</sup> The analysis is aided by the results of a series of control experiments on dodecanethiol-modified electrodes, which are used to account for the contribution of the substrate.

### Results and Discussion

The self-assembly of the 3-( $\omega$ -mercaptoundecyl)pyrrole film in ethanol was monitored by SPR, Figure 1. The final thickness of the ( $\omega$ -mercaptoundecyl)pyrrole film in ethanol is larger than expected for a single monolayer and may correspond to a bilayer film. Note that this analysis

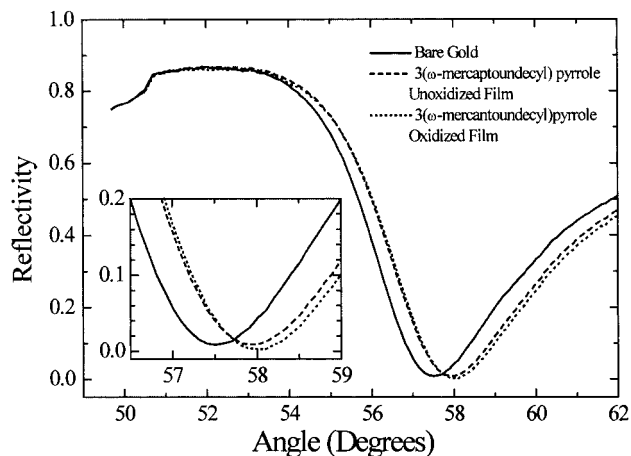


**Figure 2.** Surface plasmon resonance reflectivity vs angle of incidence. All data are obtained in the presence of ethanol with incident wavelength 632.8 nm. Shown are the data for gold after cleaning with piranha solution (solid line), after exposure to 1 mM solution of 3-( $\omega$ -mercaptopundecyl)pyrrole in ethanol for 60 h (dashed line), and after electrochemical oxidation of the 3-( $\omega$ -mercaptopundecyl)pyrrole film carried out in 0.1 M HClO<sub>4</sub> aqueous electrolyte (dotted line). Reflectance curve for the self-assembled 3-( $\omega$ -mercaptopundecyl)pyrrole film shows a shift in the reflectance minimum relative to clean gold, whereas for the oxidized 3-( $\omega$ -mercaptopundecyl)pyrrole film the data also show a change in shape, seen more clearly in the inset.

assumes the organic layer is homogeneous with an effective average dielectric constant  $\epsilon$ , of  $2.2 \pm 0.01$ , the value obtained from two-color analysis<sup>24</sup> of the fully formed film. We attribute the excess thickness to the presence of physisorbed material in addition to the chemisorbed monolayer. Rinsing with ethanol did not have an appreciable effect on the optical properties. However, if the self-assembled film is rinsed with heptane, a much better solvent, the cyclic voltammogram of the adsorbed 3-( $\omega$ -mercaptopundecyl)pyrrole film shows a  $\sim 50\%$  reduction in current drawn during in the irreversible oxidation process.

Irreversible electrochemical oxidation of the self-assembled 3-( $\omega$ -mercaptopundecyl)pyrrole film on gold was monitored by cyclic voltammetry. The first cycle shows an irreversible oxidative peak at +0.72 V vs Ag/AgCl, in agreement with the previous literature;<sup>5</sup> subsequent scans show no further oxidation.

Figure 2 shows representative SPR spectra taken in the presence of ethanol with incident wavelength 632.8 nm for bare gold (solid line), after self-assembly of the 3-( $\omega$ -mercaptopundecyl)pyrrole film but prior to electrochemical oxidation (dashed line) and finally following irreversible oxidation of the film in 0.1 M HClO<sub>4</sub> (dotted line). The SPR reflectance curve for the self-assembled ( $\omega$ -mercaptopundecyl)pyrrole film shows a shift to higher angles of the reflectance minimum relative to that of bare gold, as expected for the adsorption of a transparent thin film. In contrast, for the oxidized 3-( $\omega$ -mercaptopundecyl)pyrrole film the SPR reflectance curve shows a distinct change in shape in addition to the shift in reflectance minimum.

This change in shape of the reflectance curve is characteristic of a change in the imaginary part of the dielectric constant,  $\epsilon_{\text{imag}}$ , from a value of zero prior to oxidation (transparent film with a real dielectric constant) to nonzero after oxidation (absorbing film with nonzero imaginary part of the dielectric constant). This type of reversible switching behavior is characteristic of poly-

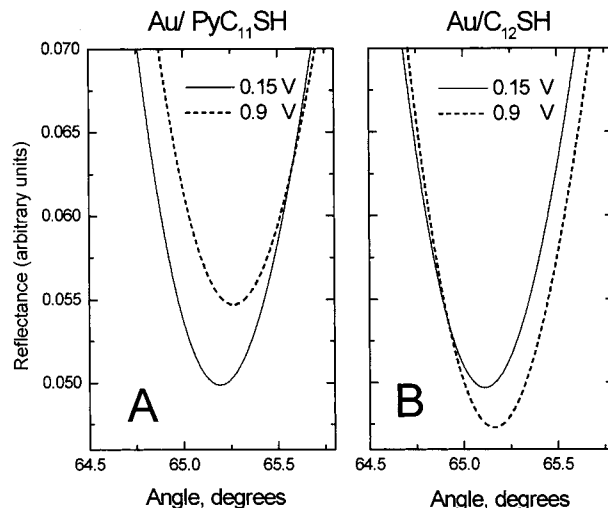


**Figure 3.** Panel A illustrates SPR results for the reproducible, reversible electrochemical cycling (after polymerization of the self-assembled ( $\omega$ -mercaptopundecyl)pyrrole film). The data cannot be interpreted without a large change in the optical constants of the organic layer upon doping. Panel B illustrates the results of control experiments on dodecanethiol films which show a small but measurable potential dependence of the SPR reflectance upon potential cycling. This is due to a change in the optical constant of the gold caused by charging of the interface and is taken into account in the data analysis (see text).

pyrrole and other conducting polymers.<sup>2</sup> We observe oxidation and reversible doping/dedoping both in aqueous perchloric acid solution and in TBAP/propylene carbonate; the effects are greater in TBAP/propylene carbonate, Figure 3A. In fact, our results indicate that a film oxidized in 0.1 M HClO<sub>4</sub> aqueous electrolyte shows an increase in  $\epsilon_{\text{imag}}$  (and conductivity, see below) upon transfer to the TBAP solution where film conductivity increases even further upon doping (roughly 50% increase).

The data represented in Figure 3A show the change in optical properties for the oxidized 3( $\omega$ -mercaptopundecyl)pyrrole film in 0.1 M TBAP/propylene carbonate and are reproducible through at least three cycles of the doping/dedoping procedure. A series of control experiments were performed measuring the SPR response of a gold surface covered with dodecanethiol to an applied potential, Figure 3B. These experiments show that the effect is not due to the underlying gold.

The optical constants of the oxidized 3( $\omega$ -mercaptopundecyl)pyrrole film layer are found to be  $2.75 + 0.9i$  and 2.7, for the doped and neutral form, respectively. The data analysis takes into account the small potential dependence of the optical constants of the gold. The dashed lines in Figure 3A are for +0.9 V vs Ag/AgNO<sub>3</sub> corresponding to the doped (oxidized) form; the solid lines are for 0 V vs Ag/AgNO<sub>3</sub> corresponding to the dedoped (neutral) form in 0.1 M TBAP/propylene carbonate. For these data, the 3( $\omega$ -mercaptopundecyl)pyrrole film was previously oxidized in 0.1 M HClO<sub>4</sub> aqueous electrolyte and then transferred to 0.1 M TBAP/propylene carbonate for the doping/dedoping study.

It is possible to extract values of the in-plane conductivity from the optical constants for the polymerized film; see theory section below. We compared our results to the effective dielectric constants calculated for published data for thick polypyrrole films from ellipsometry<sup>25</sup> and ul-

(24) Peterlinz, K. A.; Georgiadis, R. *Opt. Commun.* **1996**, *130*, 260–266.

(25) Kim, Y.-T.; Collins, R. W.; Vedam, K.; Allara, D. L. *J. Electrochem. Soc.* **1991**, *138*, 3266–75.

traviolet spectroscopy data.<sup>26</sup> On the basis of literature data, we used a bulk value of  $2.6 + 0.9i$  for the isotropic dielectric constant of a 4000 Å film and calculate a conductivity of about  $300 \text{ S cm}^{-1}$  for the oxidized form. For the oxidized monolayer films in 0.1 M  $\text{HClO}_4$  and 0.1 M tetrabutylammonium perchlorate in propylene carbonate, we calculate the in-plane conductivity to be about 23 and  $200 \text{ S cm}^{-1}$ , respectively based on our data. Most importantly, we find that film conductivity is largest for the doped state and decreases for the dedoped state.

**In-Plane Dielectric Constant and Relationship to Conductivity.** At optical frequencies, a conducting material is characterized by a complex dielectric function,  $\epsilon$ .<sup>27</sup> For light of wavelength  $\lambda$ , incident on material with conductivity  $\sigma$ , the dielectric constant can be expressed as

$$\epsilon = \epsilon_{\text{real}} + i \frac{2\sigma\lambda}{c} \quad (1)$$

where  $c$  is the speed of light. The imaginary part of the dielectric constant is thus  $\epsilon_{\text{imag}} = 2\sigma\lambda/c$ . If the dielectric constant depends on the direction of the electric field, the material will display an optical anisotropy.<sup>28</sup>

Although p-polarized light is used as the excitation source in SPR, the induced charge density wave has both longitudinal and transverse components. It is the longitudinal component which gives SPR its sensitivity to the in-plane optical properties of a dielectric film. Within the film, the longitudinal (parallel to the substrate) and transverse (perpendicular) components of the electric field are related by

$$\frac{E_{\parallel}}{E_{\perp}} = \frac{-\epsilon_{\perp} k_{\perp}}{\epsilon_{\parallel} k_{\parallel}} \quad (2)$$

In the above equation, parallel and perpendicular are defined with respect to the solid substrate;  $k$ ,  $\epsilon$ , and  $E$  denote the wave vector, dielectric function, and electric field, respectively. The wave vectors are related to the incident frequency  $\omega$  by

$$\frac{\omega^2}{c^2} = \frac{k_{\perp}^2}{\epsilon_{\perp}^2} + \frac{k_{\parallel}^2}{\epsilon_{\parallel}^2} \quad (3)$$

In the case of a very thin dielectric film, the resonant wave vector depends primarily on the dielectric properties of the metal substrate ( $\epsilon_m$ ) and the surrounding solvent ( $\epsilon_s$ )

$$k_{\parallel} \approx \frac{\omega}{c} \left( \frac{\epsilon_m \epsilon_s}{\epsilon_m + \epsilon_s} \right)^{1/2} \quad (4)$$

Combining eq 4 with eqs 2 and 3, we obtain the ratio of  $E_{\parallel}$  and  $E_{\perp}$  at the surface plasmon resonance

$$\frac{E_{\parallel}}{E_{\perp}} = \frac{-\epsilon_{\perp}}{\epsilon_{\parallel}^{1/2}} \left( \frac{\epsilon_m \epsilon_s}{\epsilon_m + \epsilon_s} \right)^{1/2} - \left( \frac{1}{\epsilon_{\perp}} \right)^{1/2} = \tan \Psi \exp(i\Delta) \quad (5)$$

The parameters  $\psi$  and  $\Delta$  are for notational convenience (see eq 7, below).

We now need to derive an effective isotropic dielectric function,  $\epsilon_{\text{isotropic}}$ , which is the parameter measured experimentally. To do this we use the electric displacement

$$\vec{\mathbf{D}} = \sum_{j=x,y,z} D_j = \sum_j \epsilon_j E_j \quad (6)$$

We substitute a value for  $\vec{\mathbf{D}}$  which applies to an isotropic film but which has the same magnitude as the  $\vec{\mathbf{D}}$  we obtain from the anisotropic treatment. If the dielectric constants are known, it is then possible to predict the value of  $\epsilon_{\text{isotropic}}$ , which will be found upon fitting experimental data to an isotropic model. Conversely, a change in the measured value of  $\epsilon_{\text{isotropic}}$  can be used to extrapolate a value of the in-plane conductivity.

The parallel (in-plane) and perpendicular (out-of-plane) components of the dielectric constant are related to the effective (isotropic) dielectric constant by

$$|\epsilon_{\text{isotropic}}|^2 = |\epsilon_{\parallel}|^2 \sin^2 \Psi + |\epsilon_{\perp}|^2 \cos^2 \Psi \quad (7)$$

where  $\psi$  is related to the ratio of the electric fields (see eq 5).

### Summary

Using SPR spectroscopy, we have shown that, upon electrochemical oxidation, self-assembled alkanethiol-pyrrole films on gold show behavior characteristic of organic conducting polymers: we observe reversible changes in the optical constants upon doping/dedoping. Optical constants are related to film conductivity; therefore, the effective isotropic dielectric constant of the film obtained in the standard SPR data analysis can be interpreted in terms of in-plane and out-of-plane contributions to film conductivity. Using this analysis, we find that the in-plane conductivity of oxidized 3-( $\omega$ -mercaptoundecyl)pyrrole is smaller, but of the same order of magnitude, than that found for thick films of polypyrrole. Most importantly, we observe reversible changes in the optical constants of the polymerized film which are consistent with electrochemical switching of an organic conducting polymer whose conductivity is largest for the doped state and decreases for the dedoped state.

**Acknowledgment.** We thank Professor David Collard of the Georgia Institute of Technology for generously providing the 3-( $\omega$ -mercaptoundecyl)pyrrole used in this work. This work was partially supported with funding from the National Science Foundation.

LA9917076

(26) Street, G. B.; Clarke, T. C.; Krounbi, M.; Kanazawa, K.; Lee, V.; Pfluger, P.; Scott, J. C.; Weiser, G. *Mol. Cryst. Liq. Cryst.* **1982**, *83*, 1285–96.

(27) Jackson, J. D. *Classical Electrodynamics*, 2 ed.; John Wiley & Sons: New York, 1975.

(28) Born, M.; Wolf, E. *Principles of Optics*, 2 ed.; MacMillan: New York, 1964.